

Glass transition in 1,4-polybutadiene: Mode-coupling theory analysis of molecular dynamics simulations using a chemically realistic model

W. Paul

Institut für Physik, Johannes-Gutenberg-Universität, Staudingerweg 7, D-55099 Mainz, Germany

D. Bedrov and G. D. Smith

Department of Materials Science and Engineering and Department of Chemical Engineering, University of Utah, 122 South Central Campus Drive, Rm. 304, Salt Lake City, Utah 84112, USA

(Received 28 April 2006; published 2 August 2006)

We present molecular dynamics simulations of the glass transition in a chemically realistic model of 1,4-polybutadiene (PBD). Around 40 K above the calorimetric glass transition of this polymer the simulations reveal a well-developed two-stage relaxation of all correlation functions. We have analyzed the time-scale separation between vibrational degrees of freedom (subpicosecond dynamics) and the α relaxation behavior (nanosecond to microsecond dynamics) using the predictions of mode-coupling theory (MCT). Our value for the mode-coupling critical temperature T_c agrees perfectly with prior experimental estimates for PBD. The predictions of MCT for the scaling behavior of the so-called β relaxation, the plateau regime separating vibrational dynamics and the α relaxation, are well fulfilled. Furthermore, we are able to derive a consistent set of MCT exponents, completely characterizing the scaling behavior of relaxation processes in the vicinity of T_c . For the temperature dependence of the α relaxation we find deviations from MCT predictions which we trace to the influence of torsional barriers on the atomic motions.

DOI: [10.1103/PhysRevE.74.021501](https://doi.org/10.1103/PhysRevE.74.021501)

PACS number(s): 64.70.Pf, 45.10.-b, 83.80.Sg

I. INTRODUCTION

Research on the structural glass transition in the last 20 years [1] has been strongly influenced by mode-coupling theory (MCT) [2]. This theory singles out density fluctuations as the relevant slow variables and describes the onset of glassy slowing down in the slightly supercooled liquid. In its idealized form MCT predicts a complete arrest of the structural relaxation at a dynamical critical temperature $T_c > T_g$, where T_g is phenomenologically defined as the temperature where the viscosity reaches 10^{13} P. The relevant length scale of the theory is the mean interparticle distance or, equivalently, the inverse of the position of the amorphous halo in the static structure factor of the liquid.

The physical picture is that in a dense liquid every particle is in a cage formed by its next neighbors. At high temperatures and low densities this cage is short lived due to the high mobility of all particles. The particle motion displays a cross-over from a ballistic regime at short times to a diffusive regime at long times when the particle has moved about the next neighbor distance. Upon lowering the temperature or increasing the density the packing constraints increase the lifetime of the cage and the particles become temporarily arrested until the cage breaks up.

In its original form the theory has been set up for simple liquids and it has been numerically solved in closed form for hard spheres [3], soft spheres [4], a binary Lennard-Jones mixture [5], and some others. Furthermore, it has been extended to simple aspherical molecules with an intramolecular orientational degree of freedom [6,7]. The only experimental system conforming to the original theoretical assumptions and forming a structural glass are sterically stabilized colloids [8]. Many structural glass formers are organic molecules or even macromolecules, and a large amount of the

experimental tests of MCT have been performed on these systems [1]. *A priori*, however, it was not clear whether and to what extent the theory would be applicable to the glass transition of, for instance, a polymer melt. It was found that molecular dynamics (MD) simulations of a bead-spring-type coarse-grained polymer model [9–12] could be consistently analyzed in terms of the predictions of MCT. For this model system this could be explained by the fact that caging sets in on a scale of monomer displacements where the connectivity within the chains is not yet felt. The connectivity could be shown to alter the late stage of the caging process (MCT β -relaxation regime). These findings motivated an extension of MCT [13] to reproduce the results of such model polymer simulations. In an MD simulation of a chemically realistic model of 1,4-polybutadiene (PBD) [14] van Zon and de Leeuw studied the scaling behavior of the structural relaxation in terms of mode-coupling predictions. Their data conformed to the temperature dependence of the α -relaxation time predicted by MCT, however with a critical temperature of 162 K, whereas the experimental T_c is 214 K. Using the same approach these authors also studied the glass transition in a polyethylenelike chemically realistic model [15]. For this model they found that the structural (α) relaxation and the late part of the β -relaxation regime for the tagged particle motion in the supercooled liquid could be consistently described by MCT. They showed that the exponent parameter of MCT [2] for their model differs from the one for the bead-spring model of Bennemann *et al.* [10] and is in better agreement with typical values found in experiments on polymers. From this, one can conclude that the form of the intramolecular potential, especially the presence of dihedral potentials, has an influence on the properties of the relaxation in the MCT regime. For the melt dynamics simulations of chemically realistic models clearly reveal the close depen-

dence of all relaxation processes on the properties of the dihedral potentials [16].

Experimentally, the glass transition in PBD has been extensively studied by a wide range of techniques, ranging from neutron scattering [17–23], to light scattering [24,25], x-ray scattering [26], nuclear magnetic resonance [27–29], dielectric spectroscopy [30–33], and dynamic mechanical response [34–36]. For PBD as well as for other glass-forming polymers some features of the glassy slowing down could be well described by MCT, but it was concluded that the caging regime could not be described consistently with MCT [37–39] in contrast to the bead-spring polymer model. The discrepancies were occurring especially in the short-time behavior, and it was argued that the lack of time-scale separation between the vibrational motion and the relaxational motion treated within MCT lies at the origin of the observed deviations.

For chemically realistic simulations of polymer melts it has been established that there exists a second mechanism for time-scale separation between vibrational and relaxational degrees of freedom besides dense packing, specifically internal rotation barriers [40]. While the presence or absence of these barriers does not affect the long-time Rouse-type dynamics of the chains [41], the dynamics on the picosecond time scale is strongly affected by the barriers. Vibrational degrees of freedom are damped out on a time scale of 1 ps, and when the typical time scale for activated barrier crossing is increased beyond about 10 ps by lowering the temperature a time window of arrested dynamics opens up. Phenomenologically this time window resembles the predictions of MCT for the glass transition; quantitatively, however, it does not conform to the predictions of the theory [40].

To understand the discrepancies between the experimental results on the glass transition in polymers and the findings from computer simulations it is important to better understand the interplay between packing constraints and the slowing down due to internal barriers as the temperature is lowered towards T_g . To this end we performed MD simulations of a chemically realistic model of PBD in the vicinity of its mode-coupling critical temperature. We will focus our analysis on the behavior of the coherent and incoherent scattering functions. The next section provides some description of our model and simulation technique. Section III presents the necessary background on MCT, and Sec. IV discusses our results. Finally we offer our conclusions in Sec. V.

II. BACKGROUND INFORMATION

A. Model and simulation technique

We will present MD simulations of a chemically realistic united atom model for PBD employing a carefully validated quantum chemistry based force field [42]. It was shown that MD simulations employing this force field are able to quantitatively reproduce experimental results on the structure and dynamics of polybutadiene melts of a random copolymer of 50% *trans*-1,4-PBD, 40% *cis*-1,4-PBD, and 10% vinyl content at elevated temperatures [43–46]. However, this force field has recently also been used to successfully model the

cis-1,4-polybutadiene homopolymer [47]. In our simulation we have 40 chains of 30 repeat units of a random copolymer of *cis*, *trans*, and vinyl groups of the above mentioned composition. We will be using a united atom model for the CH, CH₂, and CH₃ groups. The simulations are performed in the *NVT* ensemble using the Nosé-Hoover thermostat [48,49] after determining the correct density at ambient pressure for each temperature using a parallel tempering simulation.

B. Mode-coupling theory

This section will present a short summary of the results of MCT we will encounter in our data analysis [50,51]. Starting from the Liouville equation and using the Mori-Zwanzig projection operator formalism one arrives at the following formally exact equation [2] for the coherent intermediate scattering function $\phi_q(t)$:

$$\frac{\partial^2}{\partial t^2} \phi_q(t) + \Omega_q^2 \phi_q(t) + \zeta_q \frac{\partial}{\partial t} \phi_q(t) + \Omega_q^2 \int_0^t m_q(t-t') \frac{\partial}{\partial t'} \phi_q(t') dt' = 0. \quad (1)$$

Here Ω_q is a microscopic frequency scale and $m_q(t)$ is a memory kernel containing the essential physics of the problem. In the idealized version of MCT this kernel is again expressed in terms of coupled density fluctuations and the coupling constants are completely determined by the static structure of the melt. Upon lowering the temperature towards the glass transition or increasing the density this coupling induces a qualitative change in the dynamics.

In the supercooled liquid regime a two-step relaxation develops consisting of the final α or structural relaxation and a plateau or MCT- β -relaxation regime intervening between the microscopic dynamics and the structural relaxation. This β regime is the time regime of caging. Upon lowering the temperature the lifetime of the plateau (cage), t_σ ($\sigma = T - T_c$ measures the distance to the singularity), increases until it is infinite at T_c and all correlation functions only decay onto their plateau value due to vibrations within the cage. For the glass transition in the bead spring model of Bennemann *et al.* [10,12] this picture was essentially confirmed.

A central result of MCT for the behavior of correlation functions in the β regime is the factorization theorem. It states that close to T_c and in the β regime all correlation functions can be written in the following way:

$$f_q(t) = f_q^c + a_q G(t), \quad (2)$$

where f_q denotes an arbitrary intermediate-scattering function, f_q^c its plateau value, a_q an amplitude, and $G(t)$ the universal β correlator. The correlator $G(t)$ can be expanded for times close to the central β -relaxation time scale t_σ as

$$f_q(t) = f_q^c + b_q t^{-a} \quad \text{for } t < t_\sigma \quad (3)$$

and

$$f_q(t) = f_q^c - h_q t^b \quad \text{for } t > t_\sigma. \quad (4)$$

The first law is called “critical decay,” and the second one is the von Schweidler law. The exponents are determined by the so-called exponent parameter λ as

$$\lambda = [\Gamma(1-a)]^2/\Gamma(1-2a) = [\Gamma(1+b)]^2/\Gamma(1+2b). \quad (5)$$

Finally, the divergence of the α -relaxation time is determined by the exponent parameter as well:

$$\tau_\alpha \propto (T-T_c)^{-\gamma} \quad \text{with } \gamma = \frac{1}{2a} + \frac{1}{2b}. \quad (6)$$

It must be emphasized that all the above singularities hold only within the framework of the idealized MCT and then only asymptotically in the limit $\sigma = |T-T_c| \rightarrow 0$. In reality, relaxation mechanisms neglected by the idealized version of MCT become important close to T_c such that the singularities are regularized which leads to deviations from the predicted laws close to T_c as observed in simulations of the bead-spring model [10,12].

Due to the presence of these other relaxation mechanisms, there is no clear time separation between the caging time t_σ and the microscopic time t_0 present in the temperature window where the theory can be applied, such that the critical decay typically is not observable. An analysis of the β regime of MCT from simulations therefore generally focuses on the von Schweidler regime [10,12]. For our model of PBD we have analyzed the α -relaxation behavior previously [52] and have verified that this part of the relaxation processes obeys the time-temperature superposition principle. To verify this behavior it turned out to be crucial to take into account that a second relaxation regime intervenes between the vibrational dynamics and the α relaxation at low temperatures. In the following we will show that this additional regime can be consistently described by the β -regime predictions of MCT.

III. RESULTS

To get a first impression of the glassy slowing down of relaxation processes in a polymer melt it is convenient for simulations to study the mean-squared displacement (MSD) of particles:

$$\text{MSD} = \langle [\vec{r}_i(t_0 + t) - \vec{r}_i(t_0)]^2 \rangle, \quad (7)$$

where the averaging is performed over all united atoms and all starting times t_0 along the trajectory. This quantity is shown in Fig. 1 for the temperature interval $400 \text{ K} > T > 198 \text{ K}$. At high temperatures one observes a crossover from the short-time vibrational dynamics to a Rouse-like subdiffusive motion $\sim t^{0.61}$ occurring around 1 ps. Around 323 K a time-scale separation between the vibrational degrees of freedom and the relaxation behavior sets in, developing into a plateau regime in the time window between 1 and 10 ps at 253 K. The MSD arrests around 1 \AA^2 . This high-temperature time-scale separation is caused by the presence of torsional barriers along the backbone [40]. Upon lowering the temperature further, the plateau regime extends

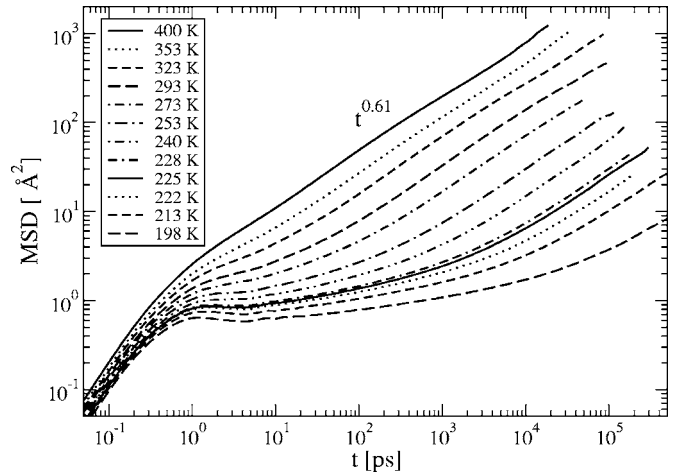


FIG. 1. Mean-square united atom displacement for temperatures indicated in the legend. At high temperatures one observes a crossover to a Rouse-like regime ($\sim t^{0.61}$); at lower temperatures a plateau regime develops due to the time-scale separation between vibrational and relaxational degrees of freedom.

up to $\approx 10 \text{ ns}$ at 198 K (if we take the time when the MSD reaches 1 \AA^2 as the extension of the plateau) and the MSD at the plateau decreases down to $\approx 0.5 \text{ \AA}^2$. Comparing these results with data for simulations of a PBD model with lowered torsional barriers [53] and with a PBD model without torsional barrier [54], both simulated at the same density as the realistic PBD, one has to assign this reduction to the reduced librational amplitude in the torsional minima. For the two lowest temperatures we see an overshoot of the MSD around 1 ps. For all temperatures this time marks the end of the vibration dominated regime [55]. Below we analyze how far the low-temperature plateau regime can be analyzed in terms of the predictions of MCT looking at the intermediate-scattering functions.

In panel (a) of Fig. 2 we show the coherent intermediate scattering function of the melt for the low-temperature range $198 \text{ K} < T < 253 \text{ K}$ at the momentum transfer q of the amorphous halo (see Fig. 8). Again one observes the development of a plateau regime starting around 1 ps, extending in time upon lowering the temperature, and increasing in amplitude. At the lowest temperature one observes oscillations superimposed on the plateau regime in a time window $1 \text{ ps} < t < 10 \text{ ps}$ which correspond to the ones seen in the MSD. Whether these oscillations indicate the presence of a boson peak [25] or are caused by finite-size effects of the simulation [56] remains to be analyzed. Panel (b) of Fig. 2 presents the time-temperature superposition of these curves [52]. For each curve time is scaled by the time the scattering functions need to decay to 0.3 which we take as a measure of the α -relaxation time at the different momentum transfers. With some deviation at the lowest temperature (198 K) we observe a superposition of the curves between 0.01 and 10 in scaled time. The master curve can be described by a Kohlrausch-Williams-Watts (KWW) law. We also note that upon lowering the temperature a clearly separable second process intervenes between the short-time vibrational decay and the α -relaxation. This process is the MCT β process we will analyze now.

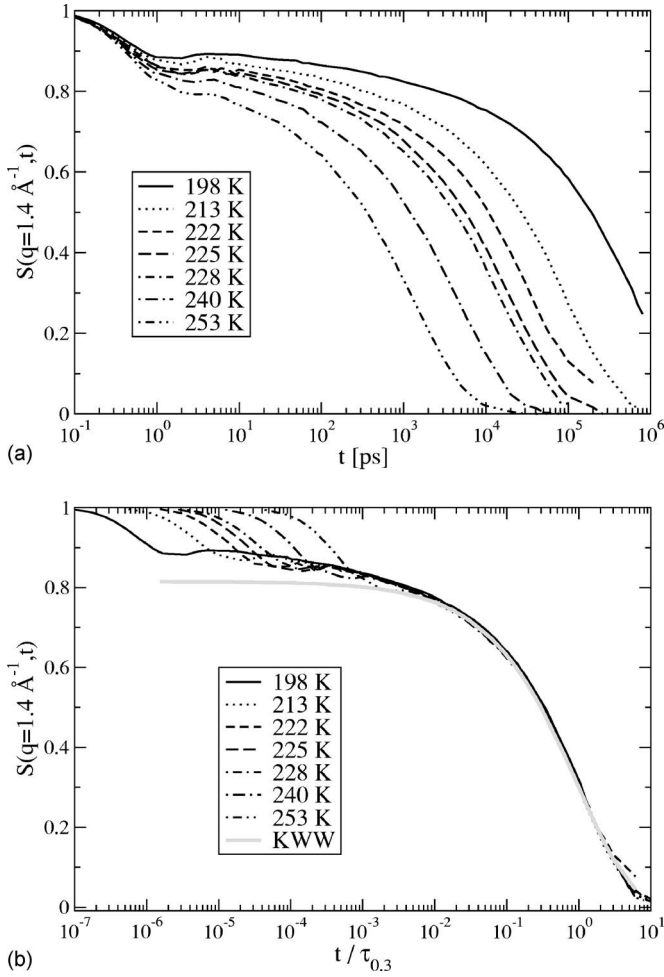


FIG. 2. Panel (a) shows the coherent intermediate-scattering function for a momentum transfer corresponding to the position of the amorphous halo ($q=1.4 \text{ \AA}^{-1}$). Panel (b) shows the time-temperature superposition of the same data as (a). The time scale of the α relaxation is approximated as the time for the curves in panel (a) to decay to a value of 0.3. Also shown in panel (b) is a Kohlrausch-Williams-Watts fit to the α relaxation (gray line).

In Fig. 3 we show incoherent intermediate-scattering functions S_{inc} for two selected momentum transfers, $q=1.4 \text{ \AA}^{-1}$ in panel (a) and $q=1.88 \text{ \AA}^{-1}$ in panel (b). The fit curves are given by extended von Schweidler laws, where we included the next-to-leading-order correction

$$S(q, t) = f_q^c - h_q t^b + h_q^{(2)} t^{2b} \pm \dots, \quad (8)$$

where $S(q, t)$ can be the coherent or incoherent intermediate-scattering function. These fits describe the decay of the scattering functions very well over quite extended time windows (10–1000 ps for 253 K and 10– 10^5 ps for 198 K). Independent of temperature and momentum transfer, the von Schweidler exponent is $b=0.3 \pm 0.01$ whereas the nonergodicity parameter f_q^c and the amplitudes h_q and $h_q^{(2)}$ depend on momentum transfer and temperature.

We find the same degree of agreement between the scattering data and the von Schweidler law for the coherent intermediate-scattering function shown in Fig. 4 for two se-

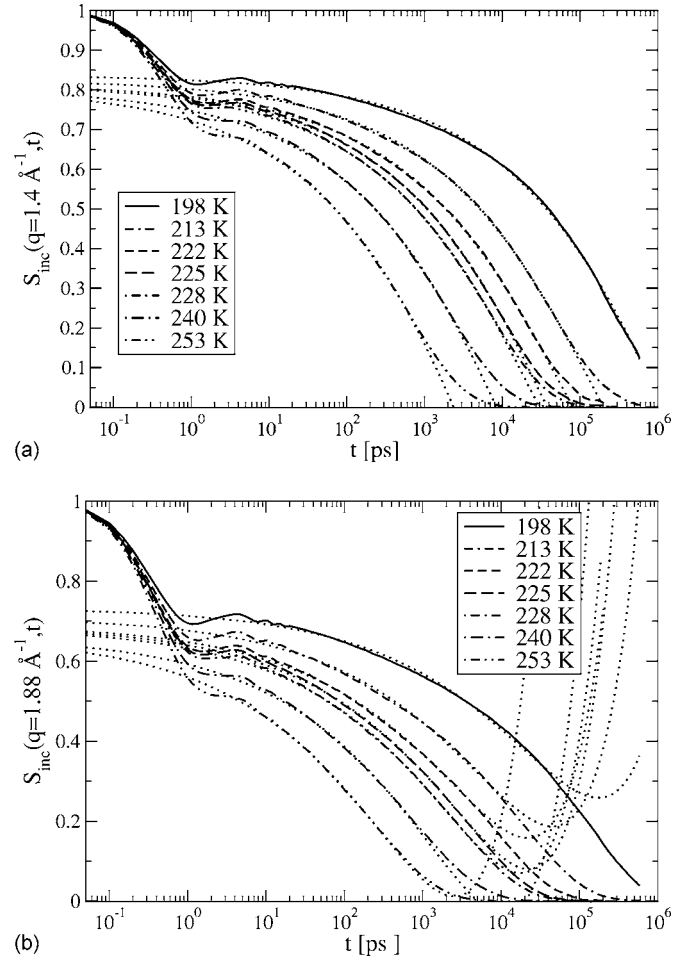


FIG. 3. Incoherent intermediate-scattering function with von Schweidler fits (dotted lines) to the plateau regime. Panel (a) is for $q=1.4 \text{ \AA}^{-1}$, panel (b) for $q=1.88 \text{ \AA}^{-1}$. The von Schweidler exponent is $b=0.3$.

lected momentum transfers. Panel (a) is for $q=1.4 \text{ \AA}^{-1}$ and panel (b) for $q=3.0 \text{ \AA}^{-1}$, the position of the second maximum in the static structure factor (see also Fig. 8), which is due only to intramolecular correlations [17,52,57]. For this large momentum transfer a large portion of the correlations decays already in the vibrational regime and the time window of applicability of the von Schweidler law is reduced. Especially at the lowest temperature of 198 K the fit is also much reduced in quality. For all the fits, however, we could use the von Schweidler exponent $b=0.3$ already found for the incoherent scattering. We can therefore conclude that the dynamic process intervening between the vibrational behavior and the structural relaxation can be fitted by the von Schweidler law predicted by MCT for all scattering functions and momentum transfer values we looked at.

If this process is the MCT β relaxation, we can further use MCT predictions to locate the critical temperature T_c . In Fig. 5 we plot the square of the amplitudes h_q of the von Schweidler laws versus temperature. MCT predicts these to be linear in the deviation from T_c . Open symbols in the figure refer to incoherent scattering data and solid symbols to coherent scattering data. The values of the momentum transfers are given in the legend. All data show a linear behavior

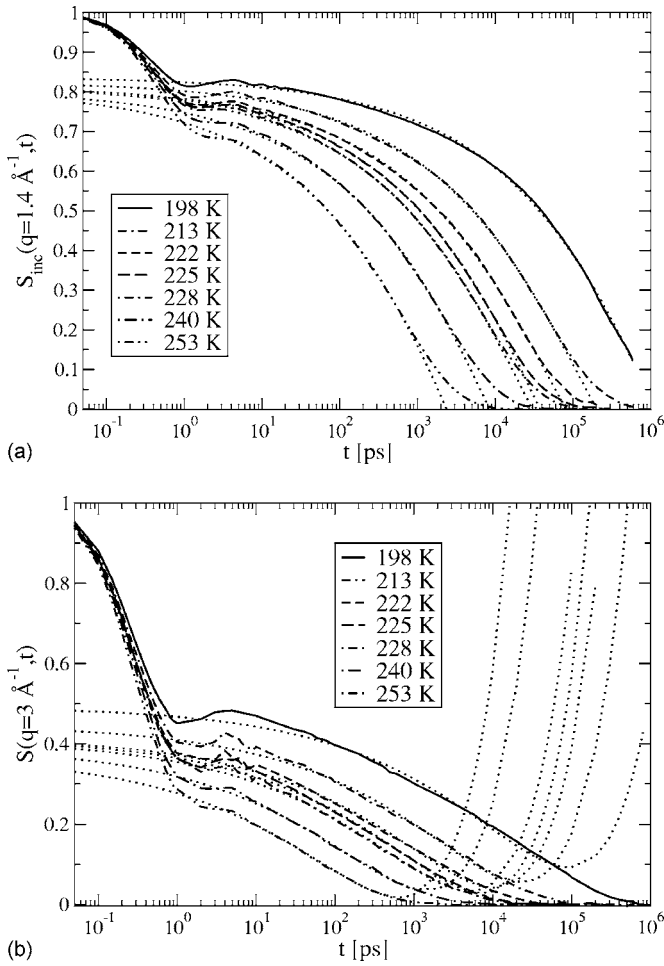


FIG. 4. Coherent intermediate-scattering function with von Schweidler fits (dotted lines) to the plateau regime. Panel (a) is for $q=1.4 \text{ \AA}^{-1}$ (position of the amorphous halo), panel (b) for $q=3.0 \text{ \AA}^{-1}$ (second peak in the static structure factor). The von Schweidler exponent is $b=0.3$, same as in Fig. 3.

for temperatures larger than 222 K. The extrapolated values of T_c lie in the temperature interval between 210 K and 218 K with an average value of $T_c=214\pm 2$ K. This value agrees excellently with the experimental value of 216 ± 1 K determined from scattering data and 214 ± 3 K determined from viscosity data [18]. We can therefore conclude that our simulation data reproduce the experimental location of the mode-coupling critical temperature and furthermore provide a prediction for the value of the von Schweidler exponent one should find in experiments—namely, $b=0.3$. Using the functional relations for the exponent parameter one can predict all other exponents from the value of the von Schweidler exponent: $\lambda=0.9$, $a=0.21$, and $\gamma=4.1$.

In Fig. 6 we show a test of the prediction of MCT for the temperature dependence of the α -relaxation times. The data are compatible with the predicted power law increase with an exponent $\gamma=4.1$ over a certain temperature window. However, this temperature window is beyond the applicability of the MCT β analysis. In the temperature range of the MCT β analysis a different power law behavior is observed with $\gamma=1.75$. Here we find significant deviations in the behavior

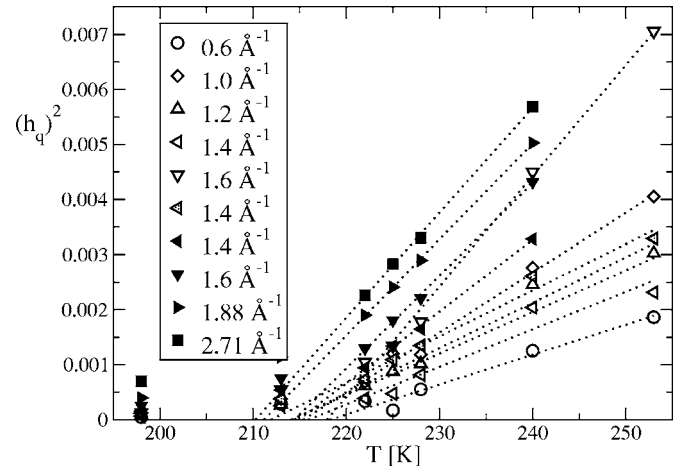


FIG. 5. Determination of the mode-coupling critical temperature T_c using the β -scaling prediction, $(h_q)^2 \sim T - T_c$, for the amplitudes in the von Schweidler laws. The average value is $T_c=214\pm 2$ K. The data shown by the left-pointing shaded triangles are obtained from the fits presented in Fig. 10.

of 1,4-PBD from the MCT predictions. We would trace these deviations to the existence of torsional barriers. We know from the high-temperature plateau regime observed in Fig. 1 that the MSD cannot increase beyond about 1 \AA^2 without the occurrence of torsional transitions [40]. If we identify the time scales when the MSD reaches this value for the different temperatures, we find, looking at the scattering functions, that these times correspond to the late β regime of MCT (the beginning of the decay from the plateau). This means that the α relaxation is determined by both physical mechanisms that lead to the vibration-relaxation separation—i.e., by packing and by torsional barriers—which we propose gives rise to the non-MCT scaling behavior observable in Fig. 6. This influence of intramolecular activation [40] was recently also worked out in a simulation of a PBD model at 200 K using a commercial force field [58].

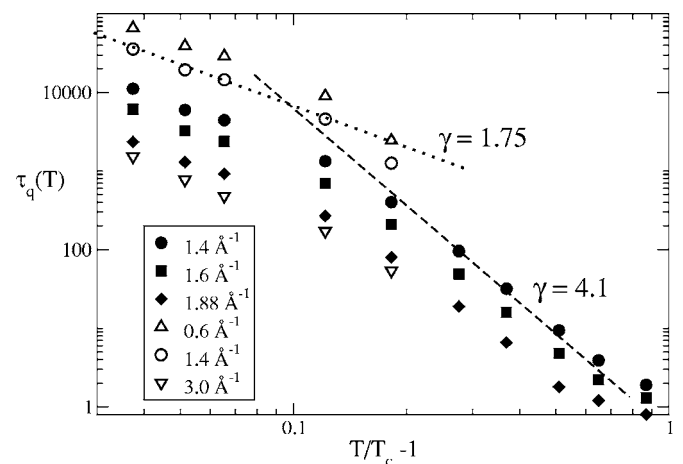


FIG. 6. Check of the MCT prediction for the scaling behavior of the α -relaxation times based on the analysis of the MCT β relaxation. The power law with exponent $\gamma=4.1$ is predicted based on the value of the von Schweidler exponent. For temperatures close to T_c a different power law regime with exponent $\gamma\approx 1.75$ is found.

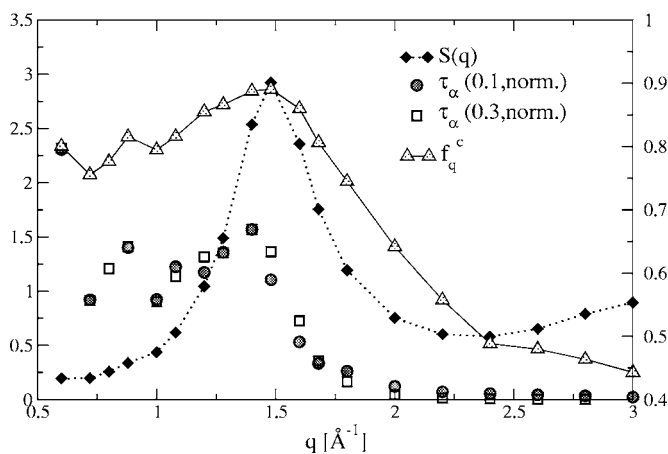


FIG. 7. Momentum transfer dependence of the static structure factor $S(q)$ (left ordinate), the α -relaxation time τ_q (left ordinate), and the nonergodicity parameter f_q^c (right ordinate) for the coherent scattering at 222 K. Two estimates of the α -relaxation time are shown: the time for $S(q, t)$ to decay to 0.3 and 0.1, respectively. These data are normalized to a value of 3/2 at $q=1.4 \text{ \AA}^{-1}$. All functions are in phase for momentum transfers smaller than the first minimum in the structure factor. The prepeaks in the relaxation time and the nonergodicity parameter are accompanied by a shoulder in the static structure factor.

In Ref. [40] we discussed that the intramolecular dihedral barriers in polymers constitute a mechanism of time-scale separation between vibrational degrees of freedom and α relaxation which acts in competition with the packing effects captured in MCT. At $T > 273 \text{ K}$ this lead to the finding that the plateau behavior in correlation functions did not follow the factorization prediction of MCT for the β regime. For lower temperatures we now find that this prediction is fulfilled, meaning that we observe a crossover from intramolecular-controlled time-scale separation (Arrhenius-like increase of the average time between torsional transitions [46]) to packing-controlled time-scale separation. Jumps may occur locally but the surrounding matrix does not yield to relax the strain imposed by the torsional jump which most often occurs through a correlated transition around a bond which is two bonds removed along the chain (for allyl bonds) [46]. This also leads to a memory effect in the local conformational structure [54] which only relaxes on the time scale of the α relaxation. While the packing effects thus are strong enough at low temperatures to generate MCT-predicted behavior in the β regime, the coupling to the conformational relaxation seems to modify the temperature dependence of the α relaxation, leading to the deviations shown in Fig. 6.

Finally we want to test the predictions of MCT for the q dependence of α -relaxation times and nonergodicity parameters. They are expected to vary in phase with the static structure factor. In Fig. 7 we have plotted the momentum transfer dependence of two measures of the α -relaxation time [time for $S(q, t)$ to decay to 0.3 and 0.1, respectively] normalized so that they agree for $q=1.4 \text{ \AA}^{-1}$ and the nonergodicity parameter together with the static structure factor for 222 K. The nonergodicity parameter varies in phase with the static structure factor over the complete momentum

range shown (up to the second maximum in the static structure factor). For the relaxation times this is only true up to the first minimum in the static structure factor. This decoupling of the momentum transfer dependence of relaxation times from the static structure factor beyond the first minimum was recently also observed in neutron scattering experiments on PBD [59]. In addition to the expected peak at the position of the amorphous halo, the relaxation times show a clear prepeak around $q=0.88 \text{ \AA}^{-1}$, which is also present in the nonergodicity parameter and shows as a shoulder in the static structure factor. This prepeak was already seen in simulations of a bead-spring polymer model [12] where it was speculated that it may occur at a momentum transfer given by $2\pi/R_g$. The physical reason for this speculation lies in the correlation hole effect in polymer melts. Within a radius of gyration around the center of mass of a polymer the density of monomers of other chains is reduced so that one can envisage a packing of fluffy, interpenetrable objects with a neighbor shell (cage size) of the order of the radius of gyration. The most prominent consequence of this structure is a subdiffusive motion of the center of mass of the polymer until it has left the correlation hole, which was found in all polymer melt simulations (for a discussion see [60]) and recently also confirmed in a comparison between simulation and experiment for PBD [45]. For the bead-spring model it was unsuccessfully tried to capture this effect by incorporating the center-of-mass structure factor into a mode-coupling description [51,61]. For our model we have $2\pi/R_g \sim 0.4$, approximately half the value at which we observe the prepeak. Whether this means that there is a different, so far unknown length scale involved or whether the deviations might be attributed to the fact that melt polymers are no spherical objects but rather adopt instantaneous configurations that look like a piece of soap, and that the dynamics is sensitive to some average of the three momenta of inertia of this geometry, is open to speculation.

We know from simulations and experiments that the second peak in the static structure factor is almost completely due to intramolecular correlations and in light of this it may not be too astonishing that the momentum dependence of the α -relaxation time in this regime is not governed by the packing effects treated by MCT. Additionally, the peak in the momentum dependence of the relaxation times is shifted with respect to the position of the amorphous halo. We attribute both of these findings to the influence of the torsional barriers on the precise behavior of the α relaxation in polymer melts, an influence which increases with increasing momentum transfer—i.e., increasing importance of intramolecular contributions to $S(q)$.

Up to this point we have analyzed the scattering functions as they pertain to the united atom model we employed for the simulation of PBD. This allowed for a direct comparison between the simulations and predictions of MCT for the glass transition. When we want to compare to experimental scattering functions, however, the scattering functions shown above give only the backbone scattering by the carbon atoms. For the experimental coherent scattering we have to calculate in addition the contributions from the deuterium atoms and the cross correlations. We have already found for PBD under pressure that these additional correlations signifi-

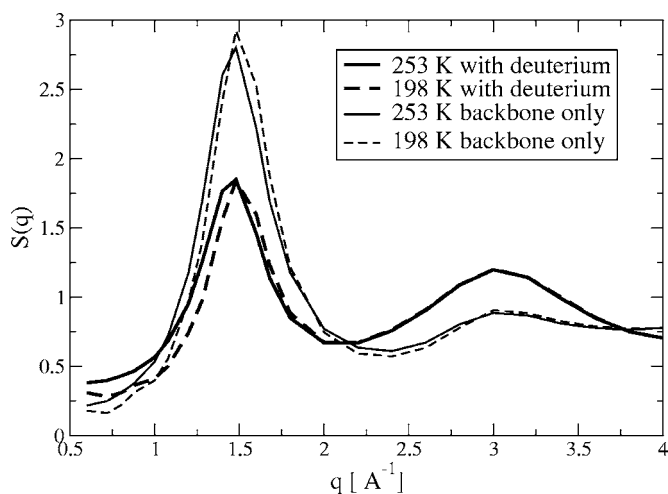


FIG. 8. Static structure factors for the united atom melt (indicated as backbone only) and after reinsertion of deuterium atoms into the simulated trajectory at their mechanical equilibrium positions (indicated as with deuterium). The positions of peaks are the same; their relative intensity, however, is strongly altered. The relative peak intensities for the curves including the deuterium scattering agree with the experimental findings.

cantly change the observable static structure factor in comparison with the pure backbone correlations [57]. In Fig. 8 we show a comparison of the static structure factor of the united atom model (indicated as “backbone only”) compared to the realistically calculated one (indicated as “with deuterium”) obtained by reinserting deuterium atoms at their mechanical equilibrium positions into the trajectory of stored united atom configurations for the two extreme temperatures for which we have analyzed the dynamics. There are two important observations to be made: the peak positions do not change between the backbone only scattering and the complete one, the peak heights, however, change significantly. Only for the calculation with deuterium is the ratio of the peak heights between the amorphous halo and second maximum comparable to experiment. On the other hand, from the complete scattering functions one would not expect the system to be anywhere close to a MCT singularity as the height of the amorphous halo is much too small. The packing effects producing the cage effect in the polymer melt only show up when the backbone correlations can be extracted separately. Only they give the strong packing correlations between the polymer strands in the melt. The complete static structure factor is strongly reduced in the regime of the amorphous halo due to destructive interference between the scattering from the carbon atoms and the deuterium atoms [57].

These additional correlations also are apparent in the coherent intermediate-scattering function, shown in Fig. 9. In panel (a) we show a comparison for fixed momentum transfer and in panel (b) at fixed temperature for selected momentum transfers. In both figures the main effect from reinsertion of the deuterium atoms is the stronger contribution of the vibrational degrees of freedom to the decay of the structural correlations, the effect increasing with increasing momentum transfer. Since the additional vibrational degrees of freedom,

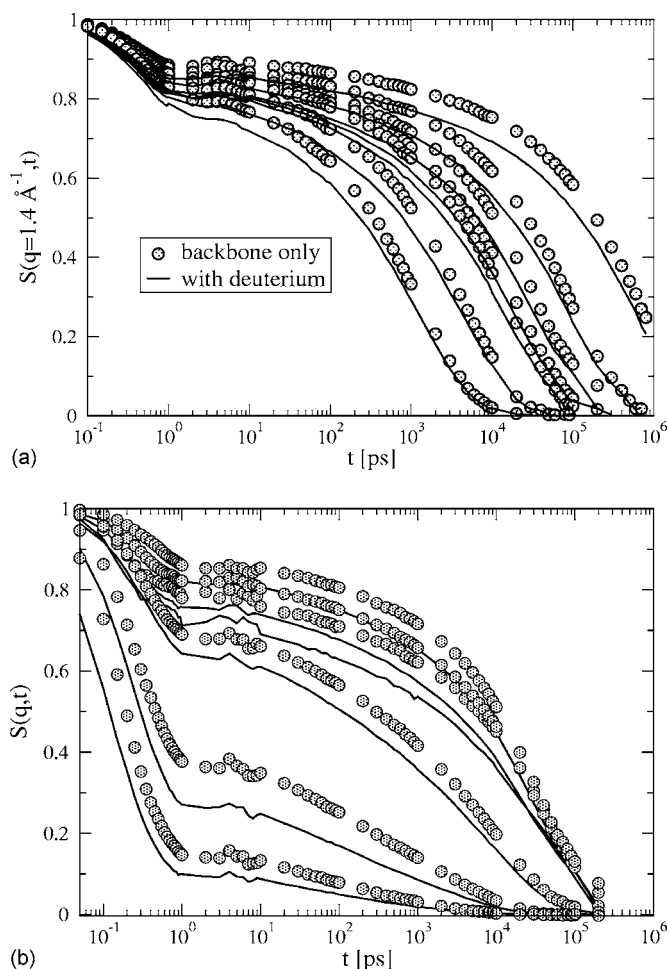


FIG. 9. Comparison of the coherent intermediate-scattering function of the simulated model (backbone only) with the ones observable in experiment (with deuterium). Panel (a) shows the comparison at fixed momentum transfer of $q=1.4 \text{ \AA}^{-1}$ for all temperatures, and panel (b) shows a comparison at fixed $T=222 \text{ K}$ for a selection of the evaluated momentum transfer values. Note that there is a stronger vibrational contribution to the short-time decay for the curves calculated with deuterium.

like, for example, the CCH angle vibrations, are not included in our simulation, this effect is caused by an amplification of the backbone motions in the displacement of the deuterium atoms which are positioned further away from the backbone. The vibrational motions involving hydrogen or deuterium atoms in the real polymer—i.e., the CCH and HCH angle and CH bond vibrations—are high-frequency motions beyond 100 THz. They would not be resolvable on the time scale of the relaxation behavior we are interested in, but might lead to an additional small increase of the decorrelation due to the vibrational motion.

Although the scattering functions shown in Fig. 9 show a clearly resolvable difference between the united atom curves and the “experimental” curves, our conclusions are not altered by this. In Fig. 10 we show the coherent intermediate scattering function for $q=1.4 \text{ \AA}^{-1}$ calculated with deuterium atoms reinserted together with von Schweidler fits to the data. Again the agreement with the scattering functions calculated from the simulation is excellent over a wide time

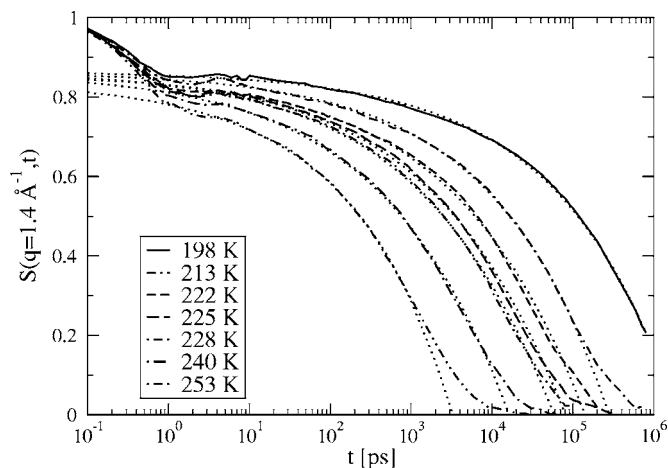


FIG. 10. Von Schweidler fits to the coherent intermediate-scattering function calculated including the contribution from the deuterium atoms. Again, the von Schweidler exponent is $b=0.3$ as in Figs. 3 and 4. The amplitude of the von Schweidler law for these fits is included in Fig. 5 and shown there with the gray left-pointing triangles.

range and again we could use the von Schweidler exponent $b=0.3$ to fit the data. Of course, the amplitude factor h_q , for instance, is different from the one determined for the backbone only scattering. The temperature dependence of this amplitude factor (included in Fig. 5 as the gray left pointing triangles), however, is compatible with a mode-coupling critical temperature $T_c=214$ K.

IV. CONCLUSIONS

We have presented in this work a molecular dynamics simulation of the glass transition in 1,4-polybutadiene employing an extensively validated, chemically realistic united atom model. We have found that upon lowering the temperature towards the calorimetric glass transition temperature of this polymer which is around 180 K, an additional process—or dynamic regime—intervenes between the short-time vibrational motion and the long-time structural relaxation. The development of this process is clearly visible when one plots the scattering functions in a time-temperature superposition form for the α relaxation. We analyzed this additional process using the predictions of mode-coupling theory for the so-called MCT β relaxation. The von Schweidler law predicted by MCT was an excellent fit to the data over a wide time and temperature window, and incoherent as well as coherent scattering functions could be fitted for all momentum transfers using a unique von Schweidler exponent $b=0.3$. From the temperature dependence of the amplitudes of the von Schweidler laws we then determined the mode-coupling critical temperature of PBD to be $T_c=214\pm 2$ K. This value is in perfect agreement with the experimentally determined one. Our value for the von Schweidler exponent can therefore be considered as a prediction for the value one should use in an analysis of experimental data on PBD.

Based on the von Schweidler exponent all other exponents of MCT can be calculated. In particular, the tempera-

ture dependence of the α -relaxation time close to T_c would be predicted to be a power law with exponent $\gamma=4.1$. One can observe a temperature window with this exponent, however not in the temperature window where we performed the β analysis where instead $\gamma=1.75$ was found. This is a clear deviation from the predictions of MCT which we trace to the presence of torsional barriers. We have shown before that torsional barriers constitute a mechanism for time-scale separation between vibrational and relaxational behavior which is present in all polymers and acts in competition with the packing mechanism treated within MCT. At low temperatures, the packing constraints are felt at smaller monomer displacements than the torsional barriers so that the plateau regime in the mean-squared displacement or the scattering functions can be consistently analyzed within MCT. In the late stages of the β regime, however, torsional transitions have to occur for the relaxation to proceed. The temperature as well as the momentum transfer dependence of the α -relaxation times therefore is not only a consequence of the β -regime behavior as stipulated by MCT but is determined by both, packing and torsional barriers.

The interplay between packing effects and intramolecular barriers also leads to deviations from MCT predictions in the momentum transfer dependence of the α -relaxation time, most notably in the q range beyond the first minimum in the static structure factor which is dominated by intramolecular correlations. An additional polymeric feature of the q dependence of the α -relaxation time seems to be a prepeak which was found in bead-spring simulations already and which we find here for PBD in a much more pronounced form.

While the analysis of the scattering functions in terms of MCT was done directly for the simulated model, contact to experiments requires calculating scattering functions after reinsertion of deuterium atoms into the simulated trajectories. Looking at the complete static structure factor from the simulation we observe a close agreement with experimental data, especially considering the relative height of the first two diffraction peaks. The fact that one is looking at a dense liquid close to its glass transition temperature is, however, lost in the experimental structure factor but inferable from the sharpness and height of the backbone structure factor. Due to the destructive interference between the carbon and deuterium scattering, the amorphous halo is significantly reduced in height and increases in width. Calculating the experimentally accessible coherent intermediate-scattering functions after reinsertion of the deuterium atoms we find that the curves lie below the backbone scattering curves for all temperatures and momentum transfers. This is mainly due to a larger contribution of the vibrational motion to the decay of structural correlations as all backbone motions get amplified for the deuterium atoms which are sticking out from the backbone. The von Schweidler law still describes the decay off the plateau in the scattering functions and the von Schweidler exponent is the one found for the backbone. The amplitudes are changed, however, their temperature dependence leads to the same critical temperature as the one determined from the backbone motion.

ACKNOWLEDGMENTS

W.P. gratefully acknowledges funding through the Materials Research Center Mainz (MWFZ) and the Forschungsfond of the University of Mainz under Grant No. 8851184.

D.B. and G.S. gratefully acknowledge support by the Center for the Simulation of Accidental Fires and Explosions funded by the U.S. Department of Energy (Grant No. B341493). G.S. is indebted to the Humboldt Foundation for support of this work.

-
- [1] *Proceedings of the Third International Discussion Meeting on "Relaxations in Complex Systems"*, edited by K. L. Ngai, E. Riande, and M. D. Ingram [J. Non-Cryst. Solids 235-237, (1998)].
- [2] W. Götze and L. Sjögren, in *Transport Theory and Statistical Physics*, edited by S. Yip and P. Nelson (Marcel Dekker, New York, 1995), p. 801.
- [3] W. Götze and L. Sjögren, Phys. Rev. A **43**, 5442 (1991); G. Foffi, W. Götze, F. Sciortino, P. Tartaglia, and T. Voigtmann, Phys. Rev. E **69**, 011505 (2004).
- [4] J.-L. Barrat and A. Latz, J. Phys.: Condens. Matter **2**, 4289 (1990).
- [5] M. Nauroth and W. Kob, Phys. Rev. E **55**, 657 (1997).
- [6] T. Franosch, M. Fuchs, W. Götze, M. R. Mayr, and A. P. Singh, Phys. Rev. E **56**, 5659 (1997); S. H. Chong, W. Götze, and A. P. Singh, *ibid.* **63**, 011206 (2001).
- [7] R. Schilling and T. Scheidsteger, Phys. Rev. E **56**, 2932 (1997); L. Fabbian, A. Latz, R. Schilling, F. Sciortino, P. Tartaglia, and C. Theis, *ibid.* **62**, 2388 (2000).
- [8] W. van Meegen, in *Transport Theory and Statistical Physics*, edited by S. Yip and P. Nelson (Marcel Dekker, New York, 1995), p. 1017.
- [9] C. Bennemann, W. Paul, K. Binder, and B. Dünweg, Phys. Rev. E **57**, 843 (1998).
- [10] C. Bennemann, J. Baschnagel, and W. Paul, Eur. Phys. J. B **10**, 323 (1999).
- [11] C. Bennemann, J. Baschnagel, W. Paul, and K. Binder, Comput. Theor. Polym. Sci. **9**, 217 (1999).
- [12] M. Aichele and J. Baschnagel, Eur. Phys. J. E **5**, 229 (2001); **5**, 245 (2001).
- [13] S.-H. Chong and M. Fuchs, Phys. Rev. Lett. **88**, 185702 (2002).
- [14] A. van Zon and S. W. de Leeuw, Phys. Rev. E **58**, R4100 (1998).
- [15] A. van Zon and S. W. de Leeuw, Phys. Rev. E **60**, 6942 (1999).
- [16] W. Paul and G. D. Smith, Rep. Prog. Phys. **67**, 1117 (2004).
- [17] D. Richter, B. Frick, and B. Farago, Phys. Rev. Lett. **61**, 2465 (1988).
- [18] B. Frick, B. Farago, and D. Richter, Phys. Rev. Lett. **64**, 2921 (1990); B. Frick, R. Zorn, D. Richter, and B. Farago, J. Non-Cryst. Solids **131-133**, 169 (1991).
- [19] D. Richter, J. Phys.: Condens. Matter **8**, 9177 (1996).
- [20] R. Zorn, T. Kanaya, T. Kawaguchi, D. Richter, and K. Kaji, J. Chem. Phys. **105**, 1189 (1996).
- [21] R. Zorn, Phys. Rev. B **55**, 6249 (1997).
- [22] A. Arbe, U. Buchenau, L. Willner, D. Richter, B. Farago, and J. Colmenero, Phys. Rev. Lett. **76**, 1872 (1996).
- [23] T. Kanaya, K. Kaji, and K. Inoue, Macromolecules **24**, 1826 (1991).
- [24] A. Aouadi, M. J. Lebon, C. Dreyfus, B. Strube, W. Steffen, A. Patkowski, and M. R. Pick, J. Phys.: Condens. Matter **9**, 3803 (1997).
- [25] A. P. Sokolov, V. N. Novikov, and B. Strube, Phys. Rev. B **56**, 5042 (1997).
- [26] D. Fioretto, U. Buchenau, L. Comez, A. Sokolov, C. Masciovecchio, A. Mermet, G. Ruocco, F. Sette, L. Willner, B. Frick, D. Richter, and L. Verdini, Phys. Rev. E **59**, 4470 (1999).
- [27] R. Dejean de la Batie, F. Laupêtre, and L. Monnerie, Macromolecules **22**, 122 (1989).
- [28] A. Guillermo, R. Dupeyre, and J. P. Cohen-Addad, Macromolecules **23**, 1291 (1990).
- [29] M. Vogel and E. Rössler, J. Chem. Phys. **114**, 5802 (2001).
- [30] R. D. Deegan and S. R. Nagel, Phys. Rev. B **52**, 5653 (1995).
- [31] A. Hofmann, A. Alegria, J. Colmenero, L. Willner, E. Buscaglia, and N. Hadjichristidis, Macromolecules **29**, 129 (1996).
- [32] R. Zorn, F. I. Mopsik, G. B. McKenna, L. Willner, and D. Richter, J. Chem. Phys. **107**, 3645 (1997).
- [33] A. Arbe, D. Richter, J. Colmenero, and B. Farago, Phys. Rev. E **54**, 3853 (1996).
- [34] R. Zorn, G. B. McKenna, L. Willner, and D. Richter, Macromolecules **28**, 8552 (1995).
- [35] S. Wartewig, I. Alig, F. Stieber, and G. Fytas, Prog. Colloid Polym. Sci. **80**, 172 (1989).
- [36] I. Alig, F. Stieber, and S. Wartewig, J. Non-Cryst. Solids **131-133**, 808 (1991).
- [37] B. Frick and D. Richter, Phys. Rev. B **47**, 14795 (1993).
- [38] R. Bergman, L. Börjesson, L. M. Torell, and A. Fontana, Phys. Rev. B **56**, 11619 (1997).
- [39] A. Kisliuk, R. T. Mathers, and A. P. Sokolov, J. Polym. Sci., Part B: Polym. Phys. **38**, 2785 (2000).
- [40] S. Krushev and W. Paul, Phys. Rev. E **67**, 021806 (2003).
- [41] S. Krushev, W. Paul, and G. D. Smith, Macromolecules **35**, 4198 (2002).
- [42] G. D. Smith and W. Paul, J. Phys. Chem. A **102**, 1200 (1998).
- [43] G. D. Smith, W. Paul, M. Monkenbusch, L. Willner, D. Richter, X. H. Qiu, and M. D. Ediger, Macromolecules **32**, 8857 (1999).
- [44] G. D. Smith, W. Paul, and D. Richter, Chem. Phys. **261**, 61 (2000).
- [45] G. D. Smith, W. Paul, M. Monkenbusch, and D. Richter, J. Chem. Phys. **114**, 4285 (2001).
- [46] G. D. Smith, O. Borodin, D. Bedrov, W. Paul, X. H. Qiu, and M. D. Ediger, Macromolecules **34**, 5192 (2001).
- [47] G. Tsolou, V. G. Mavrantzas, and D. N. Theodorou, Macromolecules **38**, 1478 (2005); G. Tsolou, V. A. Harmandaris, and V. G. Mavrantzas, J. Chem. Phys. **124**, 084906 (2006).
- [48] S. Nosé, Prog. Theor. Phys. Suppl. **103**, 1 (1991).
- [49] W. G. Hoover, Phys. Rev. A **31**, 1695 (1986).
- [50] K. Binder, J. Baschnagel, and W. Paul, Prog. Polym. Sci. **28**,

- 115 (2003).
- [51] J. Baschnagel and F. Varnik, *J. Phys.: Condens. Matter* **17**, R851 (2005).
- [52] G. D. Smith, D. Bedrov, and W. Paul, *J. Chem. Phys.* **121**, 4961 (2004).
- [53] D. Bedrov and G. D. Smith, *Macromolecules* **38**, 10314 (2005).
- [54] D. Bedrov and G. D. Smith, *Phys. Rev. E* **71**, 050801(R) (2005).
- [55] J. Colmenero, A. Arbe, G. Coddens, B. Frick, C. Mijangos, and H. Reinecke, *Phys. Rev. Lett.* **78**, 1928 (1997).
- [56] J. Horbach and W. Kob, *Phys. Rev. E* **64**, 041503 (2001).
- [57] D. Bedrov, G. D. Smith, and W. Paul, *Phys. Rev. E* **70**, 011804 (2004).
- [58] J. Colmenero, A. Arbe, F. Alvarez, A. Narros, M. Monkenbusch, and D. Richter, *Europhys. Lett.* **71**, 262 (2005).
- [59] T. Kanaya, K. Kakura, I. Tsukushi, R. Inoue, H. Watanabe, M. Nishi, K. Nakajima, K. Takemura, and H. Furuya, *J. Phys. Soc. Jpn.* **74**, 3236 (2005).
- [60] W. Paul, *Chem. Phys.* **284**, 59 (2002).
- [61] S.-H. Chong, M. Aichele, M. Fuchs, and J. Baschnagel (unpublished).